Journal of Alloys and Compounds, 182 (1992) 299–312
JALCOM 151

Ternary metal-rich Ta–Nb–S at high temperatures

Xiaoqiang Yao and Hugo F. Franzen
Ames Laboratory–Department of Energy and Department of Chemistry, Iowa State University, Ames, IA 50011 (USA)

(Received October 10, 1991)

Abstract

Two new ternary metal-rich compounds, $Nb_{21-x}Ta_xS_8$ and $Nb_xTa_{2-x}S$, isostructural with the binary metal-rich compounds $Nb_{21}S_8$ and Ta_2S respectively, were prepared by means of high temperature techniques in the ternary Ta–Nb–S system. Single-crystal structure refinements were carried out for crystals of $Nb_{21-x}Ta_xS_8$ ($R/R_w = 0.027/0.043$) and $Nb_xTa_{2-x}S$ ($R/R_w = 0.040/0.043$), and the compositions were determined as $Nb_{14.8}Ta_{6.2}S_8$ and $Nb_{0.20}Ta_{1.80}S$ respectively from the structure refinements. Stoichiometric ranges of ternary solid-solution-type metal-rich compounds found in the Ta–Nb–S system were determined. Common structural features of these metal-rich compounds are discussed.

1. Introduction

Solid state chemistry in the metal-rich region of the ternary Ta–Nb–S system is at present being explored by means of high temperature techniques. Four new ternary metal-rich compounds, $Nb_xTa_{11-x}S_4$ ($x \approx 4.92$) [1], $Nb_{12-x}Ta_xS_4$ ($x \approx 5.26$) [2], $Nb_xTa_{5-x}S_2$ ($x \approx 1.72$) [3] and $Nb_xTa_{2-x}S$ ($x \approx 0.95$) [4], have been prepared and reported. The first three compounds exhibit totally new structure types and the last one is isostructural with Ta_2Se [5] but not with Ta_2S [6]. The last two compounds are new layered compounds with van der Waals gaps consisting of neighboring sulfur layers separated by five and four mixed (Ta, Nb) layers in $Nb_xTa_{5-x}S_2$ and $Nb_xTa_{2-x}S$ respectively, in a b.c.c. setting.

Here we report the results of experiments designed to explore the composition and temperature regions of occurrence of the new phases and of solid solution regions of phases isostructural with known binary tantalum and niobium sulfides. Two new ternary metal-rich compounds isostructural with two binary metal-rich sulfides in the Nb–S and Ta–S systems, namely $Nb_{21-x}Ta_xS_8$ ($x \approx 6.2$, *I4/m*, $a = 16.817(2)$ Å, $c = 3.3450(9)$ Å, $Nb_{21}S_8$ type [7]) and $Nb_xTa_{2-x}S$ ($x \approx 0.20$, *Pbcm*, $a = 7.372(1)$ Å, $b = 5.576(1)$ Å, $c = 15.198(2)$ Å, Ta_2S type [6]) are reported. The ratios of tantalum to niobium, the temperature ranges of stabilities and some common structural features of the ternary metal-rich compounds found in this system will be discussed.

0925-8388/92/$5.00

2. Experimental details

2.1. Sample preparation

2.1.1. Initial reactants

Ta_2S was synthesized by heating a stoichiometrically appropriate mixture of tantalum (Alpha Product, M3N8), and sulfur (Fisher Scientific Company, laboratory grade) in a previously out-gassed fused silica tube at about 400 °C first, to consume all of the free sulfur, and then at 800 °C for 3 days. $Nb_{21}S_8$, NbS, "Nb_2S", "$Nb_{1.5}S$" (there are no known compounds with the formulas "Nb_2S" or "$Nb_{1.5}S$"), TaS and Ta_6S were synthesized using a similar procedure. Ta_6S was heated at 850 °C for 1 week.

2.1.2. $Nb_{21-x}Ta_xS_8$ ($Nb_{21}S_8$ type [7])

A cold-pressed sample of Ta_6S and equimolar amounts of $Nb_{21}S_8$ were arc melted three times on a water-cooled copper plate using a tungsten electrode in an argon atmosphere. The sample was subsequently annealed for 42 h at 1350 °C in an inductively heated tungsten crucible.

2.1.3. $Nb_xTa_{2-x}S$ (Ta_2S type [6])

The mixture of "Nb_2S", TaS and tantalum with $n_{Ta}:n_{Nb}:n_S \approx 1.5:0.2:1$ was pressed into a pellet, arc melted three times in an argon atmosphere and subsequently annealed at 1400 °C for 11 h in an inductively heated tungsten crucible.

2.1.4. Ternary metal-rich solid solution compounds in the Ta–Nb–S system

Preparation procedures for $Nb_xTa_{11-x}S_4$, $Nb_{12-x}Ta_xS_4$, $Nb_xTa_{5-x}S_2$, $Nb_xTa_{2-x}S$ (Ta_2Se type [5]), $Nb_{21-x}Ta_xS_8$ ($Nb_{21}S_8$ type [7]) and $Nb_xTa_{2-x}S$ (Ta_2S type [6]) are listed in Table 1.

2.2. Sample characterization

Guinier powder diffraction was used as the primary characterization method to identify phases, obtain accurate lattice parameters, and estimate the relative yields. An X-ray powder pattern was obtained with a vacuum Guinier camera FR552 (Enraf Nonius, Delft) using Cu $K\alpha_1$ radiation and silicon as an internal standard. The powder pattern of the sample was compared with the calculated powder patterns of known compounds to determine whether the desired phase was a major phase or not.

The resultant samples of the $Nb_{21}S_8$–Ta_6S mixture and "$Nb_{0.2}Ta_{1.5}S$" were examined by energy-dispersive analysis by X-rays (EDAX) in a scanning electron microscope.

2.3. Single-crystal investigation

A gray-colored single crystal ($0.4\times0.3\times0.2$ mm^3) of $Nb_{21-x}Ta_xS_8$ found in the resultant sample of the $Nb_{21}S_8$–Ta_6S and a gray-colored single crystal ($0.03\times0.01\times0.2$ mm^3) of $Nb_xTa_{2-x}S$ (Ta_2S type) found in the sample of "$Nb_{0.2}Ta_{1.5}S$" were used for X-ray intensity data collection.

TABLE 1

Summary of solid-solution-type ternary metal-rich compounds in the Ta–Nb–S system

Starting materials	Nominal compound	Heat treatments	$n_{Ta}/(n_{Ta}+n_{Nb})$	Major phase[a]	Remarks
Ta, Nb, S	$Nb_xTa_{11-x}S_4$	800 °C, 4 days Arc melting 1300 °C, 12 h	50–70% ($3.3<x<5.5$)	$Nb_xTa_{11-x}S_4$	Stable at temperatures lower than 1425 °C
Ta_6S, Nb, "Nb_2S" or "$Nb_{1.5}S$"	$Nb_{12-x}Ta_xS_4$	Arc melting	35–60% ($4.2<x<7.2$)	$Nb_{12-x}Ta_xS_4$	
TaS, Ta, "Nb_2S"	$Nb_xTa_{5-x}S_2$	Arc melting	70–80% ($1.0<x<1.5$)	$Nb_xTa_{5-x}S_2$	Thermodynamically stable at very high temperatures (at least higher than the melting point, 1450 °C), kinetically stable at temperatures lower than 900 °C
TaS, Ta, "Nb_2S"	$Nb_xTa_{2-x}S$	Arc melting	55–60% ($0.8<x<0.9$)	$Nb_xTa_{2-x}S$ (Ta_2Se type)	Thermodynamically stable at temperatures higher than 1425 °C, kinetically stable at temperatures lower than 900 °C
TaS, Ta, "Nb_2S"	$Nb_{21-x}Ta_xS_8$	Arc melting	0–30% ($x<6.3$)	$Nb_{21-x}Ta_xS_8$ ($Nb_{21}S_8$ type)	
TaS, Ta, "Nb_2S"	$Nb_xTa_{2-x}S$	Arc melting	90–100% ($x<0.2$)	$Nb_xTa_{2-x}S$ (Ta_2S type)	

[a]Characterized by Guinier X-ray powder diffraction.

Intensity data were collected using monochromatic Mo Kα radiation, employing the ω–2θ scan technique on a Rigaku AFC6 single-crystal diffractometer. The observed intensities were corrected for Lorentz polarization and absorption effects. Based on three standard reflections measured every 150 reflections for each crystal, there was no significant fluctuation or decay of the crystals. Subsequent data processing and structure calculations were performed with the program package TEXSAN. Information about intensity data collection for the two crystals is listed in Table 2.

2.3.1. $Nb_{21-x}Ta_xS_8$

After processing the intensity data, the structure model of $Nb_{21}S_8$ was used to initialize the refinement. After the refinement had converged and

TABLE 2

Crystal data for $Nb_{21-x}Ta_xS_8$ ($x \approx 6.2$) and $Nb_xTa_{2-x}S$ ($x \approx 0.20$)

Formula	$Nb_{14.8}Ta_{6.2}S_8$	$Nb_{0.20}Ta_{1.80}S$
Space group	*I4/m* (no. 87)	*Pbcm* (no. 57)
a (Å)	16.817(2)[a]	7.3724(11)[a]
b (Å)	16.817(2)[a]	5.5757(11)[a]
c (Å)	3.3450(9)[a]	15.1981(23)[a]
V (Å^3)	946.0(5)[a]	624.74(18)[a]
Z	2	12
d_{calc} (g cm^{-3})	9.665	12.029
Crystal size (mm^3)	0.4×0.3×0.2	0.03×0.01×0.2
μ(Mo Kα) (cm^{-1})	443.03	951.01
Data collection instrument	Rigaku AFC6	Rigaku AFC6
Radiation (monochromated in incident beam)	Mo Kα	Mo Kα
Orientation reflections		
number	25	12
range 2θ	14–35	14–35
Temperature (°C)	22	22
Scan method	ω–2θ	ω–2θ
Octants measured	hkl, $-hkl$	hkl, $-hkl$, $hk-l$, $-hk-l$
Data collection range 2θ (deg)	0–50	0.–70
No. of reflections measured	1045	6334
No. of unique data points, total with $F_o^2 > 3\sigma(F_o^2)$	416	581
No. of parameters refined	45	49
Transmission factors		
Maximum, minimum	1.000, 0.807	1.000, 0.350
Secondary extinction coefficient ($\times 10^{-7}$)	2.9658	0.5227
R[b], R_w[c], GOF[d]	0.027, 0.043, 1.17	0.040, 0.043, 0.911
Largest shift/esd, final cycle	0.00	0.00
Largest peak (e Å^{-3})	3.44 (0.12 Å, M6)	4.87 (1.43 Å, Ta1)

[a]Obtained from indexing of the powder pattern.
[b]$R = \Sigma\|F_o| - |F_c\|/\Sigma|F_o|$.
[c]$R_w = [\Sigma w(|F_o| - |F_c|)^2/\Sigma w|F_o|^2]^{1/2}$; $w = 1/\sigma^2(|F_o|)$.
[d]$\mathrm{GOF} = \Sigma[(|F_o| - |F_c|)/\sigma_i]/(N_{obs} - N_{parameters})$.

50% Nb and 50% Ta was assigned to each metal position, the multiplicities of the metal positions were refined. The isotropic thermal parameters were finally refined with the concomitant refinement of the multiplicities for the metal positions and the secondary extinction coefficient.

After isotropic refinement, F_c values for $Nb_{14.8}Ta_{6.2}S_8$ were calculated and used for a DIFABS absorption [8] correction for the F_0 values in the mode that utilizes θ-dependent systematic deviations $|F_0|-|F_c|$. Finally an anisotropic refinement was carried out and the final R, R_w and GOF were 0.027, 0.043 and 1.17 respectively.

2.3.2. $Nb_xTa_{2-x}S$

The space group of this compound was assumed to be *Pbcm*, the same as that of Ta_2S. First an empirical absorption correction was applied with the maximum and minimum transmission factors of 1.000 and 0.350 respectively. Application of direct methods resulted in an electron map containing four strong peaks per asymmetric unit. These peaks were assigned as tantalum and the refinement was initiated. Two sulfur positions were then obtained from a subsequent difference Fourier synthesis after initial refinements, and the multiplicities for the metal positions were refined after 50% Ta and 50% Nb was assigned to each metal position. Finally, the isotropic thermal parameters were refined with the concomitant refinement of the multiplicities for the metal positions and the secondary extinction coefficient.

After isotropic refinement, F_c values for $Nb_{0.20}Ta_{1.80}S$ were calculated and used for a DIFABS absorption correction for the F_o values in the mode that utilizes θ-dependent systematic deviations $|F_0|-|F_c|$. The ratio of the highest to the lowest transmission was 1.142. An anisotropic refinement was then carried out with the concomitant refinement of the multiplicities for the metal positions and the secondary extinction coefficient, and the final R, R_w and GOF were 0.040, 0.043 and 0.911 respectively.

3. Results

3.1. $Nb_{21-x}Ta_xS_8$ ($x \approx 6.2$)

The powder pattern that resulted from the $Nb_{21}S_8$–Ta_6S mixture could be indexed as one phase, $Nb_{21-x}Ta_xS_8$ (*I4/m*, 16.817(2) Å, 3.3450(9) Å), according to indexing accomplished using data from the structure solution for $Nb_{21-x}Ta_xS_8$ ($x \approx 6.2$) obtained in this work. Many gray-colored crystals were found in the annealed sample. The powder pattern of $Nb_{21-x}Ta_xS_8$ was similar to that of $Nb_{21}S_8$ [7] except for changes in the intensity of some reflections (the most obvious change was observed for the [110] reflection). The result of EDAX quantitative analysis of the resultant sample of the $Nb_{21}S_8$–Ta_6S mixture is as follows: 52.08 at.% Nb, 17.94 at.% Ta and 27.83 at.% S, corresponding to $Nb_{14.97}Ta_{5.16}S_8$. The composition of $Nb_{21-x}Ta_xS_8$ was determined to be $Nb_{14.8}Ta_{6.2}S_8$ from the structure refinement. The crystal data and atom coordinates for $Nb_{21-x}Ta_xS_8$ ($x \approx 6.2$) are given in Tables 2

and 3 respectively. Listing of observed and calculated structure factors for $Nb_{14.8}Ta_{6.2}S_8$ are available upon request from the authors.

The projection of the structure onto the x–y plane is included in Fig. 1. This is a solid-solution-type compound having the $Nb_{21}S_8$-type structure in which tantalum partially substitutes for niobium, *i.e.* the metal coordinations are capped pentagonal and capped cubic prismatic while the sulfur coordinations are capped trigonal prismatic. The structure can be thought of as a modified b.c.c. metal structure. The fragments of modified b.c.c. metal networks can be easily recognized from Fig. 1.

In the structure of $Nb_{21-x}Ta_xS_8$ ($x \approx 6.2$) each metal position is fractionally occupied by niobium and tantalum. The metal positions have been labeled so that, as the metal indicator increases, the n_{Ta}/n_{Nb} ratio on that position also increases, *i.e.* from M1 to M6 the n_{Ta}/n_{Nb} ratio on the metal position increases. The numbers of coordinating sulfur atoms for M1, M2, M3, M4, M5 and M6 are 4, 4, 4, 3, 2 and 1 respectively, *i.e.* there is a trend that niobium (compared with tantalum) preferentially occupies the metal site bound to more sulfur atoms.

The cell constants ($a = b = 16.817$ Å; $c = 3.345$ Å) of $Nb_{21-x}Ta_xS_8$ ($x \approx 6.2$) differ slightly from those ($a = b = 16.794$ Å; $c = 3.359$ Å) of $Nb_{21}S_8$. The radii of niobium and tantalum are nearly the same and these elements are in the same column of the periodic table, so the above similarity is not unexpected. Because the atomic positions and cell constants of $Nb_{14.8}Ta_{6.2}S_8$ and $Nb_{21}S_8$ are nearly the same, the bond distances in $Nb_{14.8}Ta_{6.2}S_8$ are nearly the same as those in $Nb_{21}S_8$.

3.2. $Nb_xTa_{2-x}S$ ($x \approx 0.20$)

The Guinier X-ray powder pattern of the arc-melted sample indicated that the major phase had a Ta_2S-type [6] structure, and a minor phase had the 2s-$Nb_{1+x}S_2$-type [9] structure. After the arc-melted sample had been annealed at 1400 °C for 11 h in an induction furnace, the powder pattern was nearly unchanged except that weak reflections from a β-Ta_6S-type compound appeared, possibly as the result of loss of sulfur during the annealing process. The cell parameters of $Nb_xTa_{2-x}S$ ($x \approx 0.20$) were determined to be $a = 7.3724(11)$ Å, $b = 5.5757(11)$ Å and $c = 15.1981(23)$ Å in the space group *Pbcm* according to indexing accomplished using data from the structure solution for $Nb_{0.20}Ta_{1.80}S$ obtained in this work.

The ratio $n_{Ta}n_{Nb}$ of the major phase in "$Nb_{0.2}Ta_{1.5}S$" was determined as 12.75, which corresponds to $Nb_{0.15}Ta_{1.85}S$, by means of EDAX quantitative analysis. The composition of $Nb_xTa_{2-x}S$ was determined as $Nb_{0.20}Ta_{1.80}S$ from the structure refinement. The crystal data and atom coordinates for $Nb_xTa_{2-x}S$ ($x \approx 0.20$) are given in Table 2 and Tables 4 and 5 respectively. A listing of observed and calculated structure factors for $Nb_{0.20}Ta_{1.80}S$ is available upon request from the authors. Figure 2 is a picture of the structure of $Nb_xTa_{2-x}S$ ($x \approx 0.20$). This is a solid-solution-type compound having the Ta_2S [6] structure type in which niobium partially substitutes for tantalum, *i.e.* the structure can be viewed as linear chains of body-centered pentagonal

TABLE 3

Positional and thermal parameters and occupancies for $Nb_{21-x}Ta_xS_8$ ($x \approx 6.2$)[a]

Atom	Occupancy	x	y	B_{eq} (Å^2)	U_{11} (Å^2)	U_{22} (Å^2)	U_{33} (Å^2)	U_{12} (Å^2)
M1	92% Nb+ 8% Ta	0.45032(7)	0.63579(8)	0.32(5)	0.0041(7)	0.00412(6)	0.0040(7)	0.0005(5)
M2	89% Nb+11% Ta	0.19231(7)	0.84247(7)	0.34(5)	0.0060(7)	0.0035(7)	0.0034(7)	0.0005(5)
M3	86% Nb+14% Ta	0	0	0.42(5)	0.0053(8)	0.0053(8)	0.005(1)	0
M4	75% Nb+25% Ta	0.27740(6)	0.98218(6)	0.32(5)	0.0037(6)	0.0042(6)	0.0042(7)	−0.0011(4)
M5	54% Nb+46% Ta	0.38325(5)	0.81483(5)	0.25(4)	0.0027(5)	0.0032(5)	0.0036(6)	0.0005(3)
M6	39% Nb+61% Ta	0.08199(5)	0.54896(4)	0.22(4)	0.0027(5)	0.0027(5)	0.0029(6)	−0.0006(3)
S1		0.2132(2)	0.6338(2)	0.2(1)	0.001(2)	0.004(2)	0.003(2)	0.000(1)
S2		0.1372(2)	0.9363(2)	0.3(2)	0.005(2)	0.002(2)	0.003(2)	0.000(1)

[a] $z = 0$; $U_{13} = U_{23} = 0$.

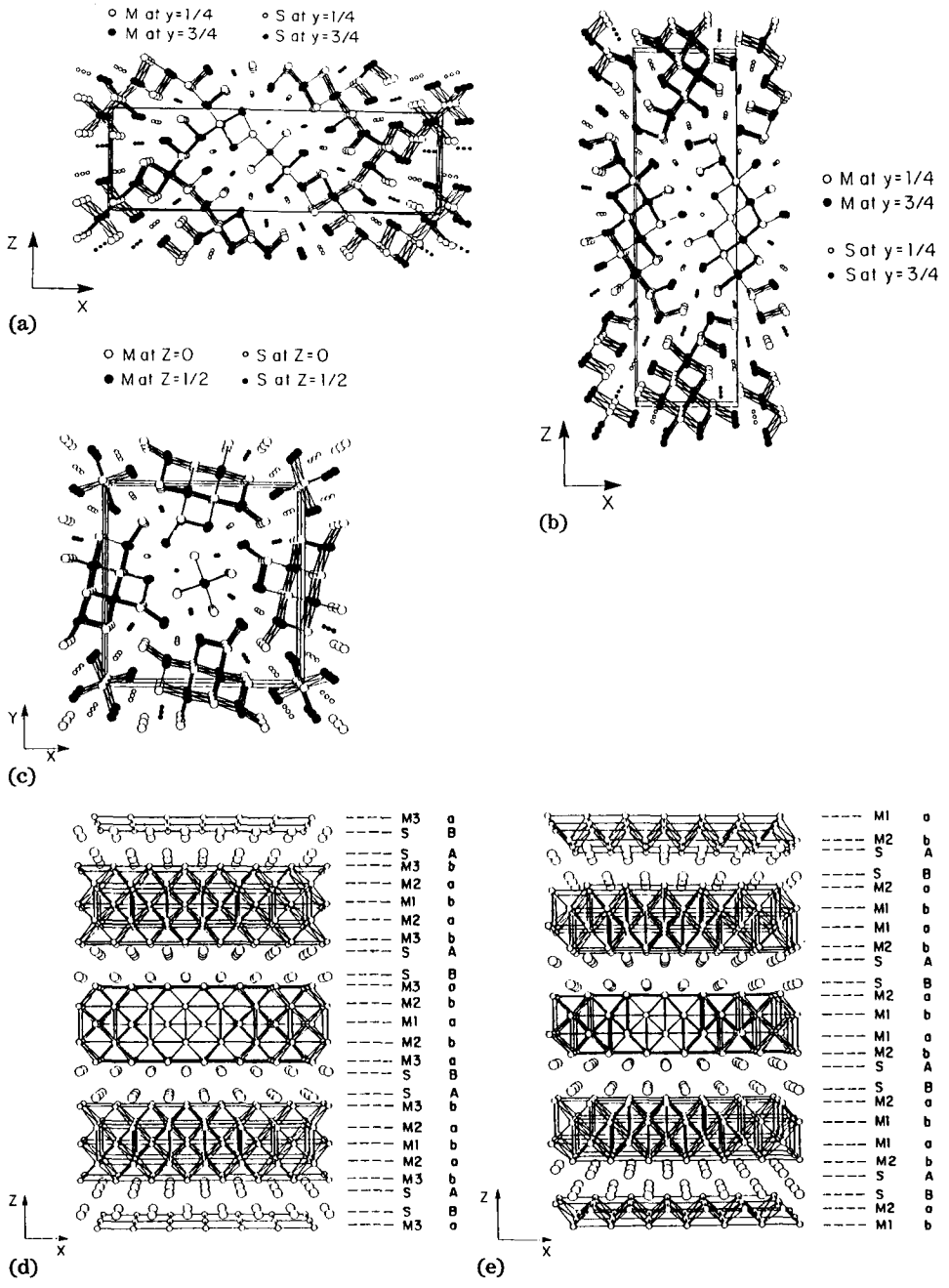

Fig. 1. Structures of metal-rich Ta–Nb–S compounds viewed along the short axis (about 3.3 Å): (a) $Nb_xTa_{11-x}S_4$ (*Pnma*; 31.210(5) Å, 3.3507(6) Å, 9.592(2) Å); (b) $Nb_{12-x}Ta_xS_4$ (*Pnma*; 9.591(3) Å, 3.364(1) Å, 32.825(7) Å); (c) $Nb_{21-x}Ta_xS_8$ ($Nb_{21}S_8$ type; *I4/m*; 16.817(2) Å, 3.3450(9) Å); (d) $Nb_xTa_{5-x}S_2$ (*I4/mmm*; 3.3203(9) Å, 21.619(12) Å); (e) $Nb_xTa_{2-x}S$ (Ta_2Se type; *P4/nmm*; 3.3304(7) Å, 9.093(9) Å).

TABLE 4

Positional and thermal parameters and occupancies for $Nb_xTa_{2-x}S$ ($x \approx 0.20$)

Atom	Occupancy	x	y	z	B_{eq} (Å^2)
Ta1		0.0084(3)	0.1320(4)	0.25	0.42(5)
M2	92% Ta+ 8% Nb	0.3523(3)	0.8715(4)	0.25	0.49(6)
M3	90% Ta+10% Nb	0.7165(2)	0.8949(3)	0.34614(7)	0.53(4)
M4	83% Ta+17% Nb	0.0964(2)	0.8941(3)	0.41025(7)	0.50(4)
S1		0.179(2)	0.25	0.5	0.6(3)
S2		0.412(1)	0.768(1)	0.4030(5)	0.9(3)

TABLE 5

Anisotropic thermal parameters (Å^2) for $Nb_xTa_{2-x}S$ ($x \approx 0.20$)

Atom	U_{11}	U_{22}	U_{33}	U_{12}	U_{13}	U_{23}
Ta1	0.0051(8)	0.0047(6)	0.0060(5)	0.0006(8)	0	0
M2	0.0068(5)	0.0057(6)	0.0065(5)	0.0000(8)	−0.0001(4)	0.0001(5)
M3	0.0074(6)	0.0073(5)	0.0053(4)	−0.0004(8)	0.0011(4)	0.003(6)
M4	0.0051(8)	0.0071(8)	0.0065(6)	−0.001(1)	0	0
S1	0.007(4)	0.014(3)	0.013(3)	−0.002(4)	0.002(3)	0.005(2)
S2	0.015(6)	0.003(4)	0.004(3)	0	0	0.001(3)

anti-prisms of metal atoms sharing faces in one direction and interconnected principally via sulfur atoms in the other two directions.

In the structure of $Nb_xTa_{2-x}S$ ($x \approx 0.20$) three out of four inequivalent metal sites are fractionally occupied by niobium and tantalum. The metal positions have been labeled so that, as the metal indicator increases, the n_{Nb}/n_{Ta} ratio on that position also increases, *i.e.* from M2 to M4 the n_{Nb}/n_{Ta} ratio on the metal position increases. The metal site where only tantalum resides is surrounded by a pentagonal anti-prism consisting only of metal atoms, *i.e.* the center columns running through the pentagonal anti-prisms of metals consist of only tantalum atoms. There are no coordinating sulfur atoms ($d_{M-S} < 3$ Å) for the metal sites surrounded by pentagonal anti-prisms of metals.

The cell constants ($a = 7.372$ Å; $b = 5.576$ Å; $c = 15.198$ Å) of $Nb_xTa_{2-x}S$ ($x \approx 0.20$) differ slightly from those ($a = 7.379$ Å; $b = 5.574$ Å; $c = 15.19$ Å) of Ta_2S. The radii of niobium and tantalum are nearly the same, so the above similarity is not unexpected. Because the atomic positions and cell constants of $Nb_{0.20}Ta_{1.80}S$ and Ta_2S are nearly the same, the bond distances in $Nb_{0.20}Ta_{1.80}S$ are nearly the same as those in Ta_2S.

3.3. Ranges of ternary metal-rich solid-solution-type compounds in the Ta–Nb–S system

Because the compounds found in this research are solid-solution-type compounds, they exist over a range instead of at a specific composition.

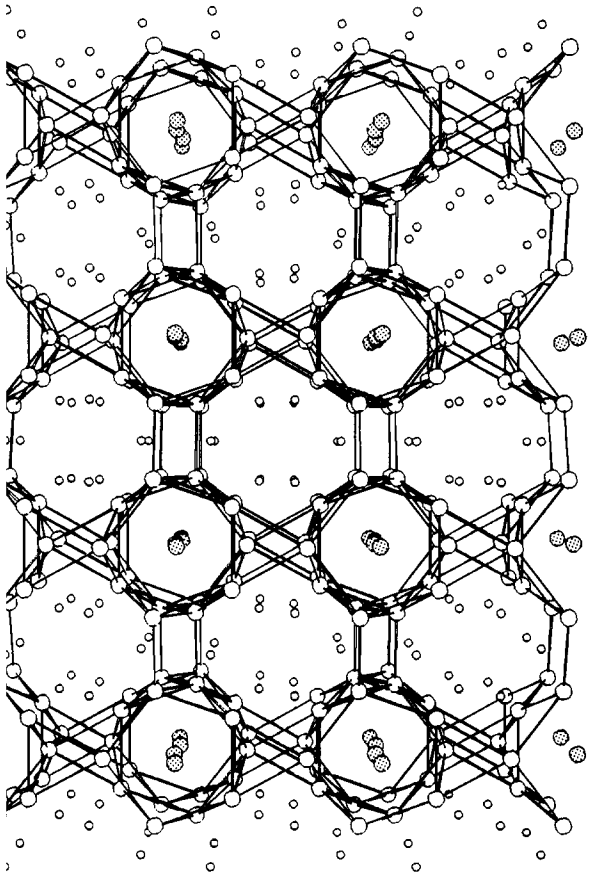

2. Structure of $Nb_xTa_{2-x}S$ (Ta_2S type; *Pbcm*; 7.372(1) Å, 5.576(1) Å, 15.198(2) Å) viewed g the *b* axis: ○, ◎, metal positions; ◎, occupied only by tantalum.

ause of the chemical and size similarities of tantalum and niobium, cell stants of $Nb_xTa_{11-x}S_4$ [1], $Nb_{12-x}Ta_xS_4$ [2], $Nb_xTa_{5-x}S_2$ [3], $Nb_xTa_{2-x}S$ ₂Se type) [4], $Nb_{21-x}Ta_xS_8$ ($Nb_{21}S_8$ type) and $Nb_xTa_{2-x}S$ (Ta_2S type) w negligible changes with x. In this research the fractions of tantalum niobium were changed while the ratio $(n_{Ta}+n_{Nb})/n_S$ was fixed at 2.75, .5, 2, 2.625 and 2 for $Nb_xTa_{11-x}S_4$, $Nb_{12-x}Ta_xS_4$, $Nb_xTa_{5-x}S_2$, $Nb_xTa_{2-x}S$ ₂Se type), $Nb_{21-x}Ta_xS_8$ ($Nb_{21}S_8$ type) and $Nb_xTa_{2-x}S$ (Ta_2S-type) re- ctively, and then ranges in which the major components (more than 90%) e of the desired phases were taken to approximate the ranges of the ɔective solid-solution-type compounds. Although the compounds found ːhis research were prepared using high temperature techniques, the ıpounds vary in their temperature ranges of stability. The results of the roximate determination of ranges of the ternary metal-rich solid-solution- ɜ compounds are listed in Table 1. In the experiments to determine the ge for each solid solution, the smallest change in $n_{Ta}/(n_{Ta}+n_{Nb})$ was 5%.

4. Discussion

When $n_{Ta}/(n_{Ta}+n_{Nb})$ is between 60 and 70% and $(n_{Ta}+n_{Nb})/n_S$ between 2 and 2.7, arc-melted samples consist of the two layered compounds, $Nb_xTa_{5-x}S_2$ and $Nb_xTa_{2-x}S$ (Ta_2Se type). Because the ranges for ternary metal-rich compounds in the Ta–Nb–S system were determined by the method mentioned above, it is difficult to know whether both of the layered compounds $Nb_xTa_{5-x}S_2$ and $Nb_xTa_{2-x}S$ (Ta_2Se type) can be formed in the above range or whether first one is formed in the range 70–80% for $n_{Ta}/(n_{Ta}+n_{Nb})$ and then the latter one is formed in the range 55–60% for $n_{Ta}/(n_{Ta}+n_{Nb})$. The same is true for the sample with ratios $n_{Ta}/(n_{Ta}+n_{Nb})$ between 50 and 55% and the ratio $(n_{Ta}+n_{Nb})/n_S$ of 2 ($Nb_xTa_{2-x}S$ (Ta_2Se type) and $Nb_{1-x}Ta_xS$ (NbS type [9]) coexisted).

The compounds $Nb_xTa_{11-x}S_4$ [1], $Nb_{12-x}Ta_xS_4$ [2], $Nb_xTa_{5-x}S_2$ [3], $Nb_xTa_{2-x}S$ [4] (Ta_2Se type [5]), $Nb_{21-x}Ta_xS_8$ ($Nb_{21}S_8$ type [7]) and $Nb_xTa_{2-x}S$ (Ta_2S type [6]) have been found in the Ta–Nb–S system using single-crystal methods. As reported previously, $Nb_xTa_{5-x}S_2$ ($x\approx1.72$) and $Nb_xTa_{2-x}S$ ($x\approx0.95$) (Ta_2Se type), as well as $Nb_{21-x}Ta_xS_8$ ($x\approx6.2$) ($Nb_{21}S_8$ type) and $Nb_xTa_{2-x}S$ ($x\approx0.20$) (Ta_2S type) were successfully refined anisotropically, while the previously reported compounds $Nb_xTa_{11-x}S_4$ ($x\approx4.92$) and $Nb_{12-x}Ta_xS_4$ ($x\approx5.26$) were refined isotropically. The crystals of the last two compounds, $Nb_xTa_{11-x}S_4$ ($x\approx4.92$) and $Nb_{12-x}Ta_xS_4$ ($x\approx5.26$), were obtained from samples melted by induction heating, while crystals of the other compounds were obtained from arc melting samples for the layered compounds $Nb_xTa_{5-x}S_2$ ($x\approx1.72$) and $Nb_xTa_{2-x}S$ ($x\approx0.95$), and from the non-melted samples for $Nb_{21-x}Ta_xS_8$ ($x\approx6.2$) and $Nb_xTa_{2-x}S$ ($x\approx0.20$). Thus the failure of the anisotropic refinements in the case of the last two compounds may stem from disorder in the solids because the samples did not crystallize well from the melt.

$Nb_xTa_{6-x}S$ with both the α-Ta_6S-type [10] and β-Ta_6S-type [11] structures were also found during the study of the ternary Ta–Nb–S system. A crystal of $Nb_xTa_{6-x}S$ (α-Ta_6S type) was found in the sample which also contained $Nb_xTa_{11-x}S_4$ [1]. The structure was refined to $R/R_w=0.191/0.249$ and the composition was determined as $Nb_{1.6}Ta_{4.4}S$. However, good quality single crystals of this compound have not yet been obtained. One possible reason is that α-Ta_6S-type and β-Ta_6S-type phases coexisted in the prepared sample, and intergrowth crystals were formed. $Nb_xTa_{6-x}S$ (α-Ta_6S type and β-Ta_6S type) can be found in the samples with $n_{Ta}/n_{Nb}>4$ and $(n_{Ta}+n_{Nb})/n_S>3$.

The structures of the known binary metal-rich sulfides Ta_2S [6], α-Ta_6S [10], β-Ta_6S [11] and $Nb_{21}S_8$ [7] in the Ta–S and Nb–S systems have been found with Nb–Ta mixtures on the metal sites, while the structures of Ta_3S_2 [12, 13] and $Nb_{14}S_5$ [14] have not yet been found among the ternary solid-solution-type compounds in the Ta–Nb–S system. Ta_3S_2 was synthesized at lower temperatures (around 1000 °C) [13], while $Nb_{14}S_5$ was difficult to obtain and was synthesized using a special procedure [14].

is not surprising that in the Ta–Nb–S system the solid-solution-type
unds $Nb_{21-x}Ta_xS_8$ ($x \approx 6.2$), $Nb_xTa_{2-x}S$ ($x \approx 0.20$) and $Nb_xTa_{6-x}S$,
ctural with the respective binary niobium-rich sulfides or tantalum-
lfides, are formed. This result is expected because of the chemical
e similarities of niobium and tantalum. What is surprising is the finding
new compounds, $Nb_xTa_{11-x}S_4$ ($x \approx 4.92$) [1], $Nb_{12-x}Ta_xS_4$ ($x \approx 5.26$)
$_xTa_{5-x}S_2$ ($x \approx 1.72$) [3] and $Nb_xTa_{2-x}S$ ($x \approx 0.95$) [4], in which the
ee exhibit totally new structure types and the last one is isostructural
$_2Se$ [5], *i.e.* the finding that these compounds are not isostructural
y known binary metal-rich compounds in the Ta–S or Nb–S system.
neral formula for the metal-rich compounds found in the Ta–Nb–S
and unknown in the respective two-component systems (Ta–S and
are M_8S_4 ($Nb_xTa_{2-x}S$ ($x \approx 0.95$)), $M_{10}S_4$ ($Nb_xTa_{5-x}S_2$ ($x \approx 1.72$)),
$Nb_xTa_{11-x}S_4$ ($x \approx 4.92$)) and $M_{12}S_4$ ($Nb_{12-x}Ta_xS_4$ ($x \approx 5.26$)).
ıen neither tantalum nor niobium is the dominant metallic element,
Ta–Nb has been shown to exhibit new structural behavior different
ither tantalum metal or niobium metal. Presumably because of the
action temperatures and the great similarities between tantalum and
ı, compounds with Nb–Ta mixtures on the metal sites were formed.
ıgments of the distorted elemental metal structures of tantalum and
ı (b.c.c.-type structure) are common features in the structures of the
unds $Nb_xTa_{11-x}S_4$, $Nb_{12-x}Ta_xS_4$, $Nb_xTa_{5-x}S_2$, $Nb_xTa_{2-x}S$ (Ta_2Se type)
$b_{21-x}Ta_xS_8$ ($Nb_{21}S_8$ type). Figure 1 shows the projections of
$_{1-x}S_4$, $Nb_{12-x}Ta_xS_4$, $Nb_xTa_{5-x}S_2$, $Nb_xTa_{2-x}S$ (Ta_2Se type) and
Ta_xS_8 ($Nb_{21}S_8$ type) onto two-dimensional planes respectively; and
gments of modified b.c.c. metal networks can be easily recognized
ig. 1. Metal–metal distances comparable with those of the nearest
ors in the elemental metal state, tantalum and niobium, were found
solid-solution-type metal-rich compounds in the ternary Ta–Nb–S
, and thus there is no doubt that there are numerous strong metal–metal
ions in these solids. These compounds are, in effect, modified in-
llic compounds in which the non-metal bonds in such a way as to
e new metal–metal interactions.
gure 3 is a plot showing the relation between numbers of coordinating
atoms and percentages of niobium for the metal positions for the
metal-rich compounds found in the Ta–Nb–S system. A general trend
served that, relative to tantalum, niobium preferentially occupies the
ositions bound to more sulfur atoms. In $Nb_xTa_{11-x}S_4$ and $Nb_xTa_{2-x}S$
ype) there were two positions, M2 (24% Nb) and M3 (28% Nb) in
$_{1-x}S_4$ and M3 and M4 in $Nb_xTa_{2-x}S$ (Ta_2S type), contradicting the
trend; these contradictions occur for the cases with the closest
ı percentages in the two metal positions in each compound and thus
nt the experimental uncertainty.
ing extended Hückel band theory the hypothetical binary Ta–S com-
isostructural with $Nb_xTa_{5-x}S_2$ [3] and $Nb_xTa_{2-x}S$ [4] (Ta_2Se type
re calculated to have lower average energies than those for corre-

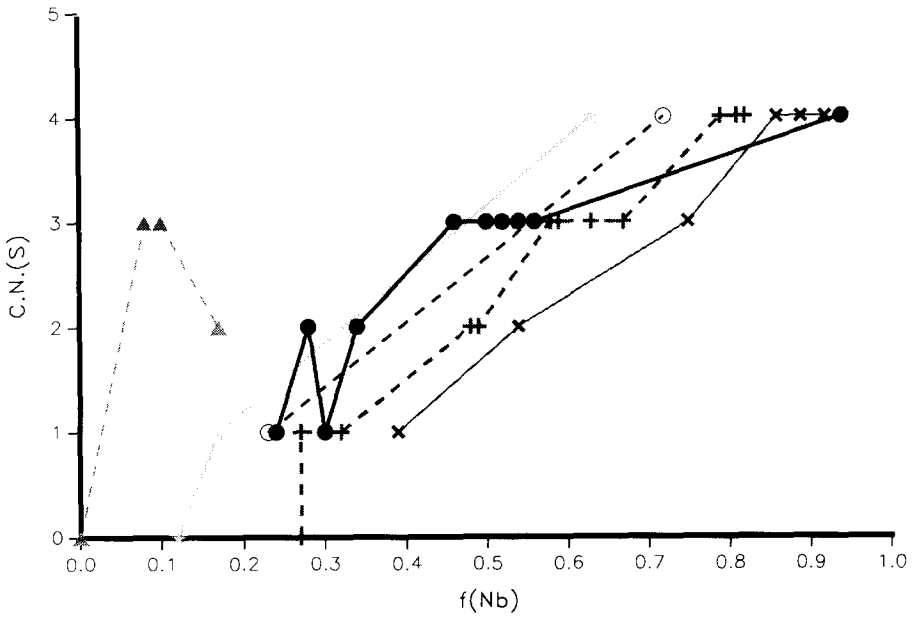

Fig. 3. Plot of the number of coordinating sulfur atoms CN(S) *vs.* fraction of niobium *f*(Nb) on metal sites for the ternary metal-rich compounds in the Ta–Nb–S system: ●, $Nb_xTa_{11-x}S_4$ ($x=4.92$); +, $Nb_{12-x}Ta_xS_4$ ($x=5.26$); ★, $Nb_xTa_{5-x}S_2$ ($x=1.72$); ○, $Nb_xTa_{2-x}S$ ($x=0.95$); ×, $Nb_{21-x}Ta_xS_8$ ($x=6.2$); ▲, $Nb_xTa_{2-x}S$ ($x=0.20$).

sponding niobium compounds, *i.e.* the Ta_xS_y binding energy is greater than that of Nb_xS_y [15].

The previously reported compounds $(Nb,Ta)_xS_y$ ($x/y=3$, 2.75, 2.5 and 2.0) establish the principle that mixed-occupancy Nb–Ta compounds can occur with stoichiometries and structures that differ from the known binaries. Here we have reported three examples ($x/y=2.625$, 2.0 and 6.0) that demonstrate that mixed occupancy on the known binary compounds is also possible. The general trend that the niobium or tantalum occupancy of a metal atom site increases as the sulfur coordination of that site increases emerged from these results. Coupled with the calculated result that Ta–S bonding is energetically more favorable than Nb–S bonding, this trend indicates the importance of metal–metal bond energy in stabilizing these compounds. It is suggested that because the Ta–S and Nb–S bond energy differences are small the configuration entropy gain drives solid solution formation, but that the energy differences do favor increased Nb–S interactions (the opposite of what would be expected naively) because those Ta–S interactions that do occur decrease the metal–metal bonding to a greater extent than the Nb–S interactions.

Acknowledgments

We thank Professor R. A. Jacobson and his group for their valuable assistance in the crystallographic portion of the study. We also express our appreciation to Dr. W. Straszheim for the EDAX analysis. This research was supported by the National Science Foundation, Solid State Chemistry, via grant DMR-8721722 and was carried out in facilities of the Ames Laboratory, US Department of Energy.

References

1 X. Yao and H. F. Franzen, *J. Solid State Chem.*, *86* (1990) 88.
2 X. Yao and H. F. Franzen, *Z. anorg. allg. Chem.*, *598* (1991) 353.
3 X. Yao and H. F. Franzen, *J. Am. Chem. Soc.*, *113* (1991) 1426.
4 X. Yao, G. J. Miller and H. F. Franzen, *J. Less-Common Met.*, in the press.
5 B. Harbrecht, *Angew. Chem., Int. Ed. Engl.*, *28* (1989) 1660.
6 H. F. Franzen and J. G. Smeggil, *Acta Crystallogr., Sect. B*, *25* (1969) 1736.
7 H. F. Franzen, T. A. Beineke and B. R. Conard, *Acta Crystallogr., Sect. B*, *24* (1968) 412.
8 N. Walker and D. Stuart, *Acta Crystallogr., Sect. A*, *39* (1983) 158.
9 F. Kadijk and F. Jellinek, *J. Less-Common Met.*, *19* (1969) 421.
10 H. F. Franzen and J. G. Smeggil, *Acta Crystallogr., Sect. B*, *26* (1970) 125.
11 B. Harbrecht, *J. Less-Common Met.*, *138* (1988) 225.
12 H. Wada, M. Onoda, *Mater. Res. Bull.*, *24* (1989) 191.
13 S.-J. Kim, K. S. Nanjundaswamy and T. Hughbanks, *Inorg. Chem.*, *30* (1991) 159.
14 H.-Y. Chen, R. T. Tuenge and H. F. Franzen, *Inorg. Chem.*, *12* (1973) 552.
15 X. Yao, G. J. Miller and H. F. Franzen, *J. Alloys. Comp.*, in the press.